

Predicting the Fuel Consumption of a Ship in Seaway Considering the Dynamic Interaction Among Environment-Hull-Propeller-Engine

Shukui Liu¹, Kah Hooi (Gerald) Beh¹ and Apostolos Papanikolaou²

Received: 17 March 2023 / Accepted: 06 August 2023
© Harbin Engineering University and Springer-Verlag GmbH Germany, part of Springer Nature 2023

Abstract

The fuel consumption of a ship has always been an important research topic, but nowadays its importance has even increased as it is directly related to a ship's greenhouse gas (GHG) emissions, which is now tightly regulated. In this paper, such a dynamic model is presented. The ship's resistance in calm water and propeller's performance in open water are required as input. The hull efficiency is estimated empirically. The diesel engine is modelled by a first-order transfer function with a delayed response and its performance is calibrated with the data from the manufacturer's catalogue. A governor is applied to maintain the pre-set engine's rotational speed and to control the engine fuel rate. A slope limiter is employed to approximate the actual engine operation during engine transients. The default values can be obtained from the manufacturer engine load acceptance diagram. The developed model is implemented in MATLAB SIMULINK environment. After validation against third-party published results, the influence of using different types of governors on ship speed and fuel consumption is investigated. The model is also applied to simulate the fuel consumption of a ship during a typical acceleration manoeuvre and the scenario of a real ship encountering harsh weather conditions.

Keywords Environment-hull-propeller-engine interaction; Fuel consumption in seaway; PI governor; Ship acceleration in harsh seaway; Marine diesel engine

1 Introduction

The fuel consumption of a ship has always been an important research topic, but nowadays its importance has even increased as it is directly related to a ship's greenhouse gas (GHG) emissions, which is now tightly regulated by IMO in its ambitious strategy fighting against climate change. A lot of studies are now being carried out on the maritime GHG emission issues (Flagiello et al., 2021;

Nahim et al., 2015; Karabulut et al., 2020; Mocerino et al., 2021; Sherbaz and Duan, 2012).

In various engineering tasks, the fuel consumption is often predicted by static models for specific operating point (s). This is very simplified and it essentially assumes an idealized steady-state condition of all the involved components, including resistance, propeller, shaft and engine, etc. Such a modelling is simple to implement but unrealistic as a ship is experiencing time-varying environmental forces and from time to time it has to conduct manoeuvres, such as acceleration/deceleration. Assuming that the seaway environment is a random process and it influences both the resistance exerted on hull and the propulsive performance of the propeller, it naturally leads to a time-varying ship speed, if the engine is operating in the constant power mode, controlled by a governor. The experienced dynamic effects lead to an increased fuel consumption compared with the steady conditions. Thus, dynamic models are needed to capture the fuel consumption of a ship in realistic environmental conditions (Kim et al., 2021).

Several studies have been conducted to investigate the dynamic effect among the hull, propeller and diesel engine. Schulten (2005) developed a system integrating multi-disciplinary sub-systems of diesel engine, ship and propeller, to examine the manoeuvring of a ship in calm

Article Highlights

- A model is presented for considering the dynamic interaction among environment-hull-propeller-engine.
- The fuel consumption of a ship is simulated during acceleration manoeuvre, and the speed performance and fuel consumption of a real ship encountering harsh weather are also simulated.
- The validation results show that the implementation of PI governor together with an acceleration slope limiter to approximate the actual engine operation during engine transients is very efficient.

✉ Shukui Liu
skliu@ntu.edu.sg

¹ School of Mechanical and Aerospace Engineering, Nanyang Technological University, Singapore

² School of Naval Architecture & Marine Engineering, National Technical University of Athens, Greece

water, to gain knowledge of the propulsion process to support the design of ship propulsion system. Bondarenko and Kashiwagi (2010) investigated the dynamic behavior of diesel engine and speed control system at off-design and transient conditions in actual seas with a view of improving the engine speed control schemes to ensure the safe operation of ship propulsion plants. They concluded that a conventional proportional-integral (PI) governor cannot effectively control the ship propulsion plant in cases of large and abrupt propeller torque losses. Taskar et al. (2016) studied the effect of waves on engine-propeller dynamics and propulsion performance of ships using a coupled model of engine and propeller along with a method to estimate wake in waves for accurate estimation of ship performance. Mizythrass et al. (2018) studied a ship’s propulsion system’s transient response during acceleration in harsh conditions using a Propulsion System Performance Simulation tool with low computational cost. A slope limiter was implemented on the diesel engine to represent the actual acceleration of the engine. Zeraatgar and Ghaemi (2019) presented a model to simulate the hull-propeller-engine interactions and analysed the effects of applying the P or PI controllers, with the objective of achieving a lower fuel consumption. The conclusion was that it would be possible for the ship to conserve a considerable amount of fuel at the cost of a slightly longer duration of voyage. Tilling and Ringsberg (2019) presented a model for the prediction of the fuel consumption of ships at sea with the motions solved in four degrees-of-freedom. To capture involuntary speed losses, engine limits are included in the model. The model was applied to study the fuel performance of alternative routes in the Baltic Sea with realistic weather forecasts. The weather routing system, as discussed in various studies, for instance, by Vettor and Soares (2016), is believed to be able to play a significant role in the future maritime transportation sector, where alternative fuels and innovative propulsion means of higher operational cost are gradually phasing in.

In this paper, a dynamic model for the simulation of a ship’s fuel consumption is presented. In this model, the ship’s resistance in calm water and propeller’s performance in open water are required as input. The diesel engine is modelled by a first-order transfer function with a delayed response and its performance is calibrated with the data from the manufacturer’s catalogue (Zeraatgar and Ghaemi, 2019). A governor is applied to maintain the preset engine’s rotational speed and to control the engine fuel rate (Bondarenko & Kashiwagi, 2010). A slope limiter is employed to approximate the actual engine operation during engine transients (Mizythrass et al., 2018). The developed model, which is implemented in MATLAB SIMULINK environment, is similar to that presented by Zeraatgar and Ghaemi (2019) except the implemented slope limiter. After validation against the results of Zeraatgar and Ghaemi

(2019) using the same case study, the tuned model is applied to simulate the fuel consumption of a ship during a typical acceleration manoeuvre and the speed/power performance of a real ship in adverse conditions. The influence of using different types of governors together with a slope limiter on ship speed and fuel consumption is investigated. This work is developed with the view of supporting the development of an advanced weather routing system (Papatzanakis et al., 2012).

2 Formulation

2.1 Ship resistance

In this study, we consider a new ship moving in calm water following a straight line. The total resistance R_T in calm water is supplied as input to the current problem.

Generally speaking, the total resistance (longitudinal force against ship’s advance) experienced by the ship at a specific steady speed V in operational condition can be described using the following equation:

$$R_{Total} = R_T + R_f + R_{AA} + \bar{R}_{AW} + R_{rud} + R_{drift} + R_{yaw} \quad (1)$$

where R_{Total} is the total resistance acting on a ship in seaway, R_T the total resistance of a new ship in calm water, R_f the resistance due to fouling development on hull surface, R_{AA} the mean added resistance due to relative wind, \bar{R}_{AW} the mean added resistance due to waves, R_{rud} the resistance due to rudder action, R_{drift} the hull drifting forces in the steady condition, R_{yaw} the added resistance due to yaw motion, etc.

2.2 Propeller characteristics

The propeller open-water performance is typically provided in the form of K_T-K_Q-J curves, which are supplied as input to the current problem.

When a ship is navigating at speed V , the advance velocity u_A can be calculated as:

$$u_A = V(1 - w) \quad (2)$$

where w is the wake fraction. The advance coefficient is defined as follows:

$$J_A = \frac{u_A}{n_p \cdot D_p} \quad (3)$$

Obtaining the advance coefficient, we can calculate the resulting values of K_T and K_Q from the open-water characteristics of the propeller. The thrust generated by the propeller and the required torque are then calculated as follows:

$$T = K_T \cdot \rho \cdot n_p^2 \cdot D_p^4 \quad (4)$$

$$Q_p = K_Q \cdot \rho \cdot n_p^2 \cdot D_p^5 \quad (5)$$

where T is the produced thrust, Q_p is the propeller torque, n_p is the number of propeller shaft revolutions per unit time and D_p is the propeller diameter.

The wake fraction and thrust deduction fraction required in the simulation can be supplied based on experimental or numerical results. If no data is provided, they can be estimated using the following empirical expressions (Molland et al., 2011):

$$w = -0.05 + 0.5C_B \text{ (Taylor)} \quad (6)$$

$$t = 0.5C_p - 0.12 \text{ (Hecker)} \quad (7)$$

Finding the thrust produced by the propeller, the net thrust can be derived by factoring in the thrust reduction factor as follows:

$$T_N = T(1 - t) \quad (8)$$

It should be noted that during ship operation, both the ship speed V and the propeller speed may change with time, therefore resulting in an instantaneous change in the advance coefficient J_A . Furthermore, the values of the wake fraction w and the thrust reduction fraction t will also change with ship operation.

2.3 Diesel engine

The diesel engine's torque as a function of fuel consumption is modelled as a 1st order transfer function with time delay (Xiros, 2002; Zeraatgar & Ghaemi, 2019), which takes the form as follows:

$$\frac{Q_E(s)}{h(s)} = e^{-\tau s} \cdot \frac{K_E}{1 + T_E \cdot s} \quad (9)$$

where h is the fuel input to the engine, τ is the time delay of the system, K_E is the gain of the engine, and T_E is the time constant. The engine torque $Q_E(s)$ is the output of the system. These can be calculated using the equations shown below:

$$\tau = \frac{1}{2 \cdot Z_E \cdot n_E} \quad (10)$$

$$T_E = 0.9 \frac{2\pi}{\omega_E} \quad (11)$$

$$K_E = \frac{Q_E(n_{E0})}{h(n_{E0})} \quad (12)$$

where Z_E is the number of engine cylinders, ω_E and n_E are the angular velocity in rad/s and rate of engine shaft revolutions in rev/s, respectively, and n_{E0} is the engine shaft revolutions at Normal Continuous Rating (NCR). The Specific Fuel Oil Consumption (SFOC) curve of the engine is

required to calculate the fuel rate h . The fuel rate is modelled based on the SFOC curve and the dynamic behaviour of this equipment is not taken into account.

2.4 General equations relating hull, propeller and engine

For a ship advancing on a straight line at speed V , the resistance exerting on the hull is denoted as R_{Total} and the propulsor provides a net thrust T_N to overcome the resistance. When the net thrust T_N is larger than the total resistance R_{Total} of the ship, the ship will accelerate and this motion can be described following Newton's Second Law:

$$T_N - R_{\text{Total}} = (\Delta + a_{11}) \dot{V} \quad (13)$$

where Δ is the displacement of the ship and a_{11} is the added mass in the longitudinal direction. The ship's added mass is a function of the ship's geometry and it can be estimated numerically by using a potential theory seakeeping 3D panel code (Liu & Papanikolaou, 2012) or be approximated empirically (e.g., Korotkin, 2008). Estimated values by potential theory, are in general between 2% to 5% of ship's mass, depending on the slenderness of the hull. It proved recently, while calculating the added mass of a catamaran by CFD (Xing-Kaeding and Papanikolaou, 2021) that the effect of viscosity on the estimation of a_{11} is significant and should not be neglected.

Similarly, we have the equation which relates the torque generated by the engine shaft and required by the propeller, namely, Q_E and Q_p , respectively. When the engine torque is larger than the propeller torque, the shaft will be accelerated and this can be described as follows:

$$Q_E - Q_p = (J_p + J_{\text{added}}) \cdot \dot{\omega}_p \quad (14)$$

where ω_p is the angular velocity of the propeller; J_p is the propeller moment of inertia and can be approximated as follows:

$$J_p = \frac{D_p^2}{k_p} \cdot m_p \quad (15)$$

where m_p is the mass of the propeller and k_p is a value typically between 19~28, often cited as 23.

The added moment of inertia of the propeller can be approximated using the empirical formula of MacPherson et al. (2007) as:

$$J_{\text{added}} = C_{\text{IE}} \cdot \rho \cdot D^5 \quad (16)$$

$$C_{\text{IE}} = C_1 \cdot \text{EAR} \cdot \frac{p}{D} - C_2 \quad (17)$$

where EAR and p/D are the expanded area ratio and pitch ratio of the propeller, respectively. And the empirical values of the C_1 and C_2 coefficients are presented in Table 1.

Table 1 Coefficients used in calculating C_{IE}

Coefficients	Z = 3	Z = 4	Z = 5	Z = 6
C_1	0.004 77	0.003 94	0.003 59	0.003 44
C_2	0.000 93	0.000 87	0.000 80	0.000 76

2.5 Engine’s governor and calculation of fuel index

Modern marine diesel engines are always equipped with a speed governor to maintain a certain commanded speed and to limit its operation within some constraints. A governor does this by computing the fuel rate input and controls the fuel actuator, while considering the limitations of the engine such as the maximum torque (Altosole and Figari, 2011). This is especially important when the engine is operating near the engine limits, or when the environment that the ship is operating in induces large propeller load variations. Therefore, the governor is crucial to ensure that the propulsion plant of the ship functions smoothly and safely (Lanchukovsky, 2009).

In this study, we will use a PI-type governor provided by MATLAB-Simulink to carry out the simulations. A PI-type governor comprises action from both Proportional (P) control and Integral (I) control. P-control is the simplest form of feedback control and works by linearly correlating the controller output to the input signal. However, it tends to yield a bias signal, or steady-state error, thus preventing the system from achieving the steady-state set point. This behaviour is described as follows:

$$c(t) = K_p \cdot e(t) + b \tag{18}$$

where $c(t)$ is the controller output, K_p is the proportional gain of the controller, $e(t)$ is the error signal and b is the bias.

In contrast to P-control, I-control is able to remove the bias and return the system to the intended state. A negative input signal will cause the I-controller to return a decreasing signal, whilst a positive input signal will cause the signal to increase. However, the I-controller alone is much slower than the P-controller despite its accuracy. The behaviour of the I-controller is described as follows:

$$c(t) = K_I \int e(t) dt + c(t_0) \tag{19}$$

where K_I is the integral gain of the controller and $c(t_0)$ is the controller output before integration.

By combining both P- and I-controls, the bias is removed, and the speed of the controller is ensured. The equation for PI-control is as follows:

$$c(t) = [K_p \cdot e(t) + K_I \int e(t) dt] + c(t_0) \tag{20}$$

In this study, we will follow the Ziegler-Nichols method (Ellis, 2012) to tune the K_I and K_p parameters of the controller.

The output signal of the governor is defined as $m(t)$ in

the time domain. It is used to calculate the change in fuel index, ΔX_f , as follows:

$$\Delta X_f(t) = \frac{m(t)}{n_{ss}} \tag{21}$$

where n_{ss} is the rotational speed of the shaft at steady-state conditions. This represents the dynamically changed increment of the fuel index. As the output of the governor changes when the ship is accelerating, $\Delta X_f(t)$ would be changing as well.

The fuel index at the current time, X_f , which is the operating point of the engine, is then changed by the value ΔX_f :

$$X_f(t) = X_{f,ss} + \Delta X_f(t) \tag{22}$$

Therefore, the governor combines the dynamic increments of the fuel index with that of the steady state fuel index to return a new fuel index. The new fuel index will give us the new fuel rate, h , which can be determined by:

$$h = X_f(t) \cdot FR_{SMCR} \tag{23}$$

where SMCR is the specified maximum continuous rating.

3 Numerical implementation

The above outlined method has been implemented in MATLAB Simulink environment, as schematically presented in Figure 1.

When a higher speed is specified/commanded, the error signal to the PI governor, which is the difference between the commanded speed and the actual/current engine speed, will increase. Based on the gain settings of the governor, the output will be adjusted accordingly to reduce the error input. In this case, the change in fuel index, $\Delta X_f(t)$ will be increased to supply more fuel into the diesel engine. Subsequently, the diesel engine will supply more torque to increase the engine shaft revolutions. For a direct-drive configuration, the propeller revolution rate will be the same as the engine shaft revolution rate. Therefore, the advance number will decrease, resulting in an increase in the thrust and torque coefficients, thereby increasing the net thrust and the propeller torque simultaneously. The increase in net thrust results in the ship undergoing acceleration, and the ship speed to increase with time. The increase in propeller torque results in lower net torque available to accelerate the engine shaft revolutions, therefore decreasing the acceleration. The increase in ship speed results in an increase in the ship resistance, leading to an increase in the effective power. Subsequently, the required brake power and the operating point of the engine is ramped up, which will determine the new steady-state fuel input to the engine. After this, the cycle repeats with the new error signal

Table 3 Simulation result from Case 1

K_p	Total time (s)	Fuel consumption (kg)
1	1 344.6	1 012
2	1 297.4	1 100
3	1 287.6	1 117
4	1 283.4	1 124
5	1 281.2	1 127
6	1 279.8	1 129
7	1 278.8	1 131
8	1 278.2	1 132
9	1 277.6	1 132
10	1 277.2	1 133
11	1 276.9	1 133
12	1 276.6	1 134
13	1 276.4	1 134
14	1 276.2	1 135
15	1 276.1	1 135
16	1 275.8	1 135
17	1 275.5	1 134
18	1 275.2	1 134
19	1 275.0	1 134
20	1 274.8	1 134
21	1 274.6	1 134
22	1 274.5	1 134
23	1 274.3	1 135
24	1 274.2	1 135
25	1 274.1	1 135
26	1 274.0	1 135
27	1 273.9	1 135
28	1 273.8	1 135
29	1 273.7	1 135
30	1 273.6	1 136
31	1 273.6	1 136
32	1 273.5	1 137
33	1 273.4	1 138

As for the results of Case 2, we can deduce that there is no significant difference in travelling time or fuel consumption due to the addition of the I-controller. This is because the I-controller works to counteract the effects of the P-controller, when the P-controller has caused the system to overshoot the intended point. The I-controller thus works to bring the system back to the intended steady-state value, and this effect can be seen below in the following figures. While there are no significant differences across different values of K_p , the value of the optimal K_i of the PI-controller is determined according to the Ziegler-Nichols method and is taken to be 1.2 times of the frequency at $K_p = K_{max} + 1$. Figure 2 shows the oscillations when the system is unstable, and the period of oscillations is 0.52 s. The optimal value of K_i is therefore calculated to be 2.31.

Table 4 Simulation result from Case 2, $K_p=14.85$

K_i	Total time (s)	Fuel consumption (kg)
1	1 274.0	1 137
2	1 274.0	1 137
3	1 274.0	1 137
4	1 274.0	1 137
5	1 274.0	1 137
6	1 273.9	1 137
7	1 273.8	1 137
8	1 273.8	1 137
9	1 273.8	1 137
10	1 273.8	1 137
11	1 273.8	1 137
12	1 273.8	1 137
13	1 273.8	1 137
14	1 273.8	1 137
15	1 273.8	1 137
16	1 273.8	1 137
17	1 273.8	1 136
18	1 273.8	1 136
19	1 273.7	1 137
20	1 273.7	1 137
21	1 273.7	1 137
22	1 273.7	1 136
23	1 273.7	1 136

The optimal values of the PI-controller, namely, $K_p=14.85$ and $K_i=2.31$, are then used in the following simulations.

As can be seen in Figure 3, when the full-ahead command is given, the engine’s actual speed undergoes a very fast increase in revolution rate and reaches 103 r/min within 1 s, while it reaches the steady state value of 92.8 r/min rapidly thereafter. This shows the engine overcompensating for the step increase in commanded speed, and may result in a waste in fuel consumption as the fuel input to the engine is increased by a large amount.

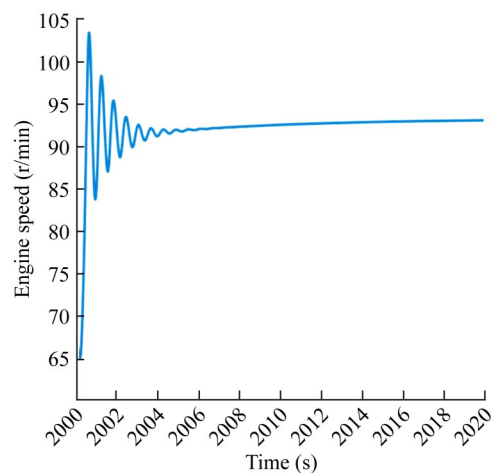


Figure 3 Time-history of engine speed (r/min)

Figures 4–6 show the obtained time-histories of the concerned characteristics, including the instantaneous ship speed, the distance travelled, and the total fuel consumption of the ship with respect to time.

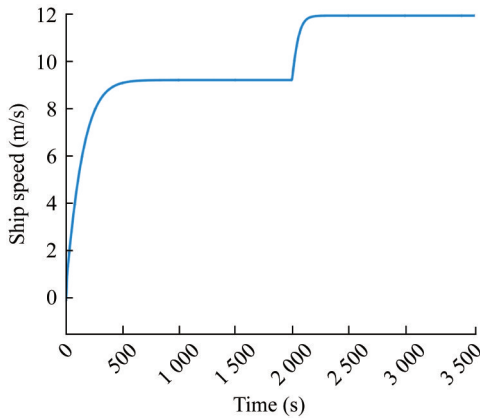


Figure 4 Time-history of ship speed V

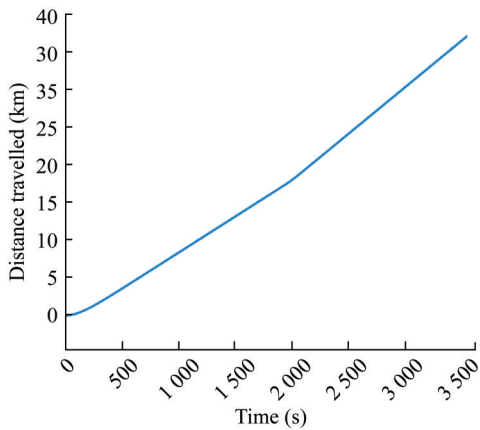


Figure 5 Time-history of distance travelled by ship

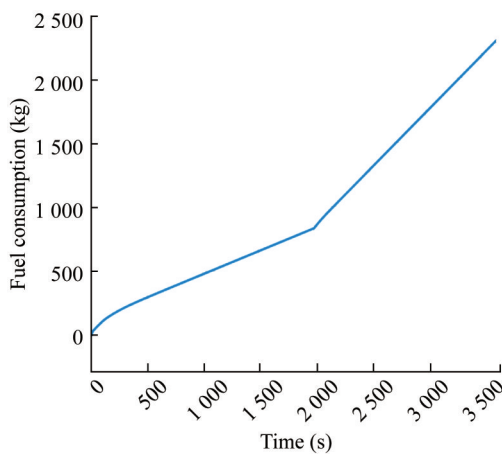


Figure 6 Time-history of fuel consumption

We observe in Figure 7 a significant difference between T_N (in red) and R_T (in blue) as the ship undergoes acceleration after $t=2\ 000$ s for over 200 s. This is owing to the

large inertia/mass of the ship, which results in a long time required to bring the ship to the desired speed. While a large net thrust is required to accelerate the ship, the large inertia of the ship results in a very low acceleration. This results in a much higher fuel consumption compared with the case of reduced net thrust supplied to bring the ship to speed at a slower rate. In Figure 8, we also observe a much higher engine torque supplied as opposed to the propeller torque for the initial 2 s of ship acceleration. While this difference exists for a shorter duration compared with what is observed in Figure 7, the significant difference between the two torques account for the sudden increase in the engine speed shown in Figure 3. Similarly, in Figure 9, the delivered brake power is much higher than the required brake power for several hundred seconds starting from $t = 2\ 000$ s. This tells us that a high acceleration of the engine speed would result in an excessive power output, subsequently a much higher fuel consumption rate throughout the acceleration phase, which will be further discussed in the following section.

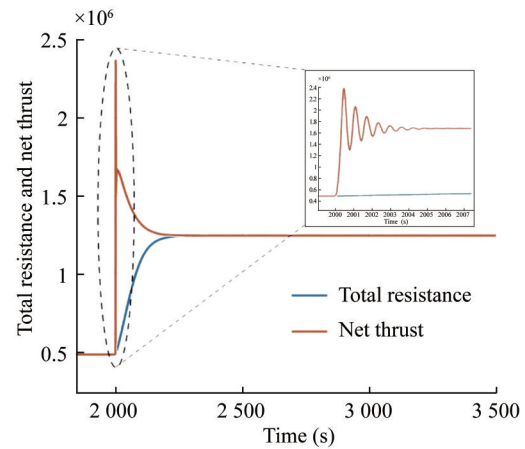


Figure 7 Time-history of total resistance (R_T) and net thrust (T_N)

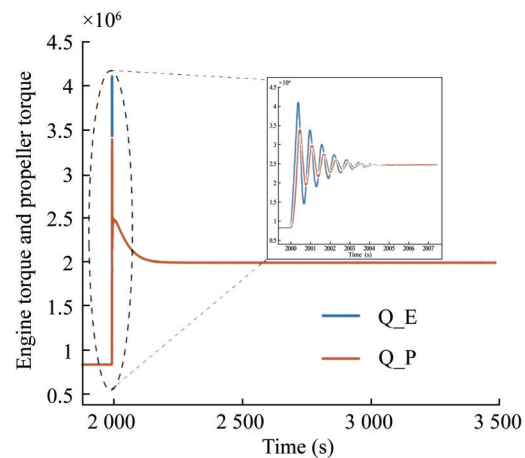


Figure 8 Time-history of engine torque (Q_E) and propeller torque (Q_P)

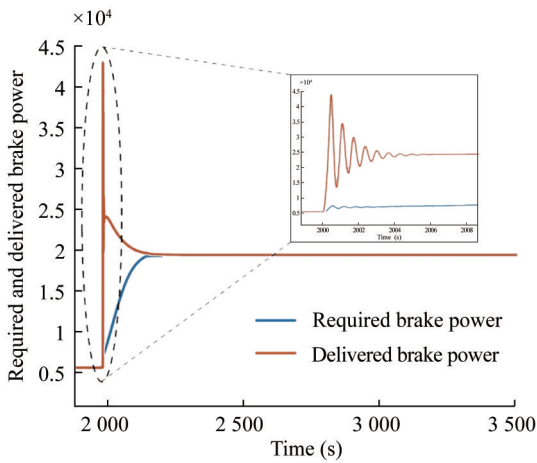


Figure 9 Time-history of required and delivered brake power

In order to further examine the influence of the P Controller, a case study was conducted by setting the integral gain to 0. Figure 10 shows the simulated shaft revolutions when the proportional gain $K_p=1$ and $K_i=0$. As can be seen, the shaft experiences an instantaneous jump in the revolution rate at $t=2\ 000$ s, which is not realistic. The revolution rate then gradually increases to the setpoint, over a period of approximately 800 s. When compared with results shown in Figure 3 using a PI-controller, this case takes significantly longer duration, which indicates that the engine is unable to respond quickly to command, and may not be desirable in maneuvering at sea. This “lag” in engine acceleration and therefore, ship speed, also explains the difference in time taken for the ship to travel 15 km as compared to a ship under the action of a PI controller. It is also observed that the difference between the Net Thrust T_N (in red) and Total Resistance R_T (in blue) over time is much smaller, as shown in Figure 11, when compared with the scenario in the previous sub-section where a PI controller is used. This is due to the milder acceleration of the shaft to the steady-state value, and therefore there is a lower fuel consumption in this case, as pointed out by Zeraatgar and Ghaemi (2019).

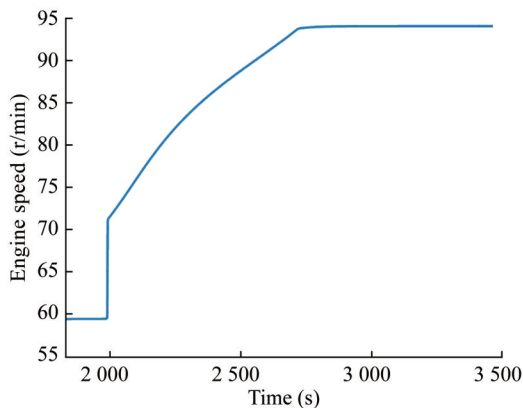


Figure 10 Time-history for engine speed for Case 1, $K_p=1$

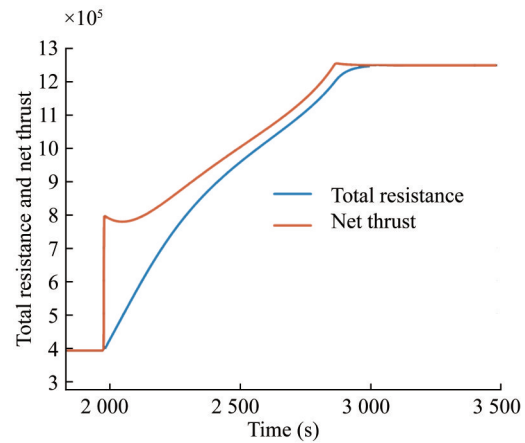


Figure 11 Time-history of total resistance (R_T) and net thrust (T_N) with P-controller, $K_p=1$

Figure 12 shows a comparison of the achieved engine speed when using PI or P governors. When the model is first initialised for 65 r/min, the P governor is unable to bring the engine speed to the desired setpoint, and when the step input of 92.8 r/min is given, the engine speed overshoots without returning. Therefore, steady-state errors will exist when using a P-controller. This is in contrast to the PI governor, which is able to reach the desired setpoint very accurately. Note that PI-controllers are used in the maritime industry to control the main engines.

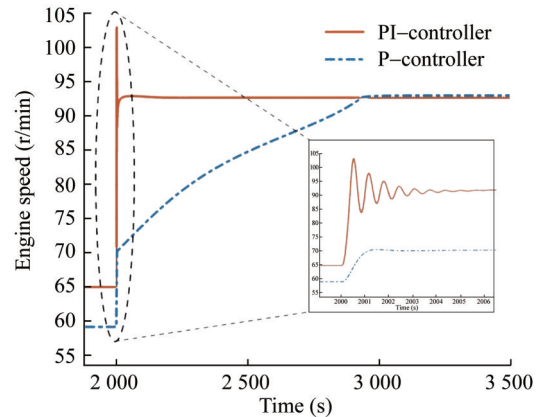


Figure 12 Comparison of engine speed when using P or PI governor

When using PI-controller, the diesel engine accelerates almost instantaneously, from 65 r/min to 101 r/min when a new speed is commanded, as shown in Figure 3, and the input power is increased from 30% to 100%. Such a situation is highly improbable and undesirable as such a high acceleration in engine revolutions would place high stress on the shaft and result in thermal overload of the engine, leading to damages and risks. Normally, an engine load limiter is implemented in the governor to control the rate of increase in shaft revolutions, as also indicated in the engine manufacturer’s publications (MAN Diesel & Turbo,

2016). As such, a slope limiter for the ordered engine speed can be employed to represent the actual engine operation, as shown in the study of Mizythras et al. (2018). In this study, we implement the same settings of the speed slope limiter in the governor. With the slope limiter, the engine acceleration is limited to 0.04 r/min/s in the simulation from 65 r/min to 92.8 r/min when the input power is increased from 30% to 100%, as shown in Figure 13. As a result, the target engine speed is achieved in over 700 s, which is more realistic than what has been observed in the simulations without a slope limiter. As the engine accelerates at a slower, controlled rate, the ship speed increases at a slower rate, taking 800 s to reach the steady-state speed, as shown in Figure 14. This results in a longer time to complete the travelling distance of 15 km and the fuel consumption during this voyage also decreases, as shown in Figures 15 and 16, respectively.

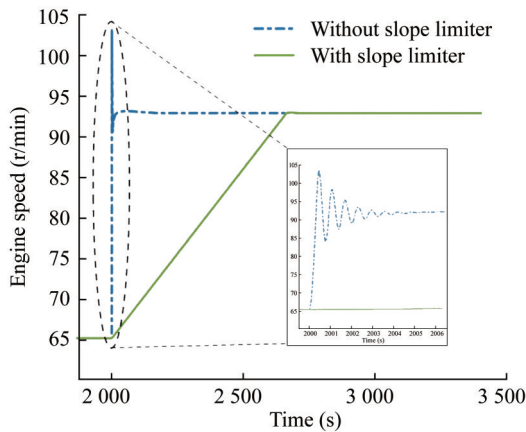


Figure 13 Time-history of engine speed with slope limiter, together with a PI governor

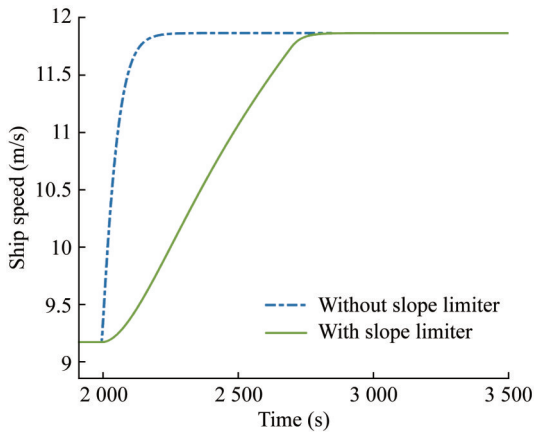


Figure 14 Time-history of ship speed with slope limiter

Figures 17 and 18 present the comparison of the net thrust and the total resistance, as well as the delivered engine power and the hydrodynamic power required by the propeller, obtained with or without the acceleration limiter being implemented. When an acceleration limiter is ap-

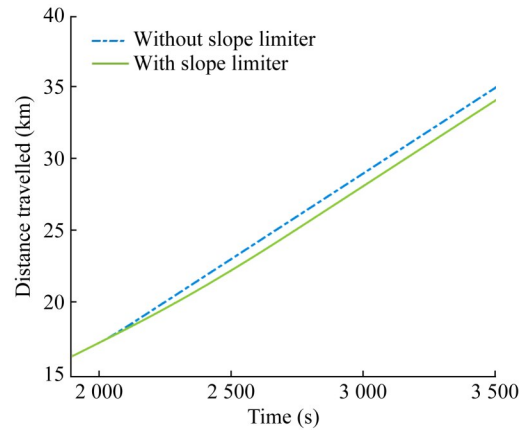


Figure 15 Time-history of distance travelled with slope limiter

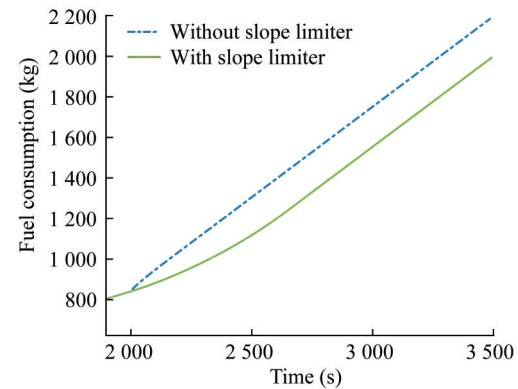


Figure 16 Time-history of fuel consumption with slope limiter

plied, it takes the ship a much longer time to achieve at the steady-state. During this process, the difference between the net thrust and the total resistance, as well as between the delivered brake power and the required hydrodynamic power, is much smaller when the limiter is applied. Subsequently, a mild acceleration is observed and less fuel is consumed. This is in line with manufacturer’s instruction on engine operation during acceleration manoeuvre (MAN Diesel & Turbo, 2012).

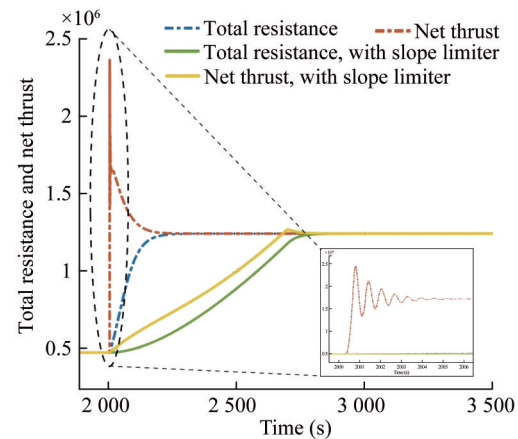


Figure 17 Time-history of total resistance (R_T) and net thrust (T_N) with slope limiter

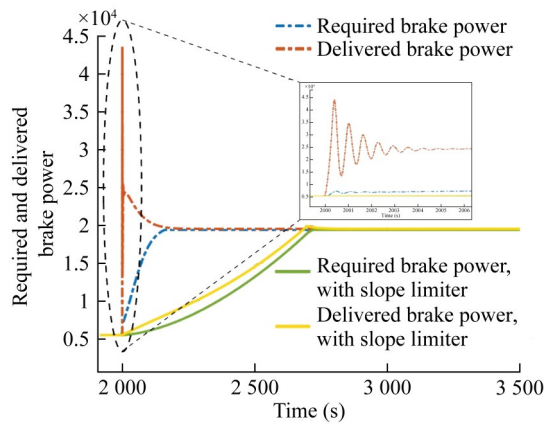


Figure 18 Time-history of required and delivered brake power with slope limiter

Table 5 shows the results of the simulations conducted with the slope limiter, compared alongside the results without the use of the slope limiter. Evidently, the results with the slope limiter show a decrease in fuel consumption with a less than proportional increase in total time. This is given that the slope limiter reduces the engine speed acceleration, resulting in less fuel input to the engine. When $K_f = 2.31$, the fuel consumption with the limiter is 1 002 kg, as compared with the 1 137 kg without the limiter, demonstrating a 12% decrease. However, by limiting the acceleration, the total time taken for the ship to travel 15 km increases by 74 s, which is about 6%. Still, the time taken to travel 15 km decreases less proportionally than the increase in fuel consumption to make good this time. Therefore, it can be concluded that the use of the slope limiter is indeed beneficial in terms of fuel consumption for a ship undergoing acceleration.

Figure 19 shows the engine load, in terms of its power output and the shaft speed, plotted (in blue) in the engine operating envelope, as described by Klein Woud and Stapersma (2002). Clearly, the engine load curve lies to the left of the propeller load curve during the acceleration process, which demonstrated the dynamic interaction among hull, propeller and engine during ship acceleration.

5 Application to realistic scenario

Given that the model is able to account for the dynamic interactions of the hull-propeller-engine, the model is then applied to analyse the scenario that a ship encounters an adverse seaway condition. This is a realistic scenario, particularly related to the safe navigation of bulk carriers and tankers (IMO, 2021; Liu et al., 2022a).

A product carrier is selected for this case study. Its main features are list in Tables 6 and 7, and the resistance curve and open-water characteristics are presented in Figures 20 and 21, respectively. From the onboard monitored data, it

Table 5 Simulation result from Case 2, $K_p = 14.85$

K_f	Without slope limiter		With slope limiter	
	Total time (s)	Fuel consumption (kg)	Total time (s)	Fuel consumption (kg)
1	1 274.0	1 137	1 348.1	1 002
2	1 274.0	1 137	1 348.2	1 002
3	1 274.0	1 137	1 348.2	1 002
4	1 274.0	1 137	1 348.2	1 002
5	1 274.0	1 137	1 348.2	1 001
6	1 273.9	1 137	1 348.2	1 001
7	1 273.8	1 137	1 347.8	1 005
8	1 273.8	1 137	1 347.7	1 005
9	1 273.8	1 137	1 347.7	1 007
10	1 273.8	1 137	1 347.6	1 008
11	1 273.8	1 137	1 347.5	1 009
12	1 273.8	1 137	1 347.5	1 009
13	1 273.8	1 137	1 347.5	1 010
14	1 273.8	1 137	1 347.5	1 011
15	1 273.8	1 137	1 347.4	1 012
16	1 273.8	1 137	1 347.4	1 013
17	1 273.8	1 136	1 347.4	1 014
18	1 273.8	1 136	1 347.4	1 015
19	1 273.7	1 137	1 347.4	1 016
20	1 273.7	1 137	1 347.3	1 016
21	1 273.7	1 137	1 347.2	1 017
22	1 273.7	1 136	1 347.1	1 017
23	1 273.7	1 136	1 347.0	1 018

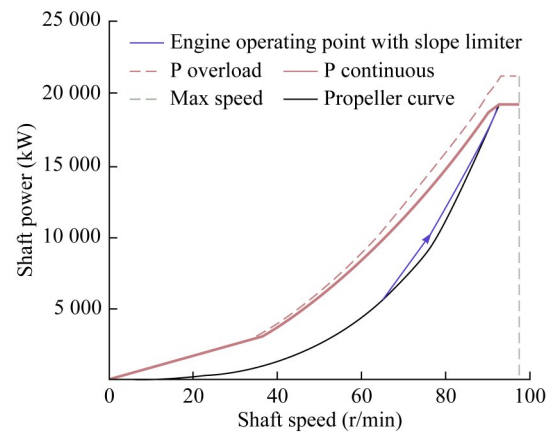


Figure 19 Engine load during ship acceleration

was noted that the ship encountered a harsh weather condition with 18 m/s wind and waves of significant height of 4.45 m in 2017. As the model requires the engine speed as input, the monitored engine speed is adopted as input. Figure 22 shows such a scenario where the engine speed

drops from 118 to 92 within 45 minutes. A linear behaviour is assumed as the best approximation of the monitored data (one point per 15 minutes). During the simulation, the fouling, wind and wave effects are considered, and the increase in resistance and drop in propeller efficiency are predicted (Liu & Papanikolaou, 2020 & 2023; Liu et al., 2022b), as shown in Figure 23. Figure 24 shows the engine power output from the simulation and Figure 25 shows the ship speed drops from about 14 kn to approximately 2.75 kn during this process. Following the concept of the minimum propulsion power assessment, if a ship can maintain a minimum speed of 2 kn in adverse conditions, then she can be manoeuvred efficiently to avoid any dangerous situation. The simulation results thus proves that the subject ship disposes the propulsion and steering abilities for safe navigation in adverse conditions.

Table 6 Ship characteristics

Parameter	Value
Displacement, Δ (t)	54 574.01
Length BP, L_{BP} (m)	174
Beam, B (m)	32.26
Mean draft, T (m)	11.7
Propeller diameter, D_p (m)	5.971
Number of blades, Z	4
Area ratio, EAR	0.4
Pitch ratio, P/D	0.7
Engine speed at SMCR, n_{E0} (r/min)	121
Number of cylinders, Z_E	6
Power at SMCR, $P_{B,SMCR}$ (kW)	9 000

Table 7 Engine characteristics (MAN B&W 6S50MC-C)

Load (%)	Speed (r/min)	SFOC (g/kWh)	FR (kg/s)
10	56.2	189.0	0.043 050
20	70.8	175.0	0.079 722
30	81.1	170.9	0.116 782
40	89.3	168.4	0.153 431
50	96.2	165.8	0.188 828
60	102.3	163.5	0.223 450
65	105.1	162.6	0.240 738
70	107.7	162.0	0.258 300
75	110.2	162.1	0.276 921
80	112.6	162.5	0.296 111
85	114.9	163.1	0.315 780
90	117.1	164.0	0.336 200
95	119.3	165.1	0.357 258
100	121.0	166.3	0.378 794

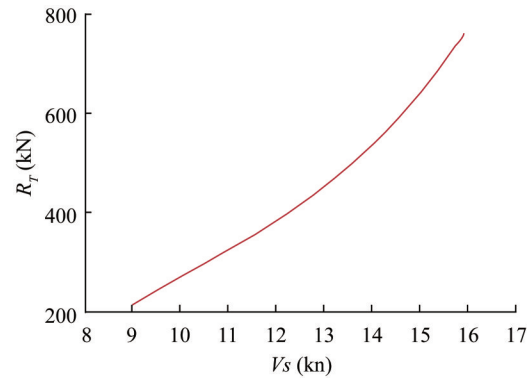


Figure 20 Resistance curve of the subject ship under design conditions

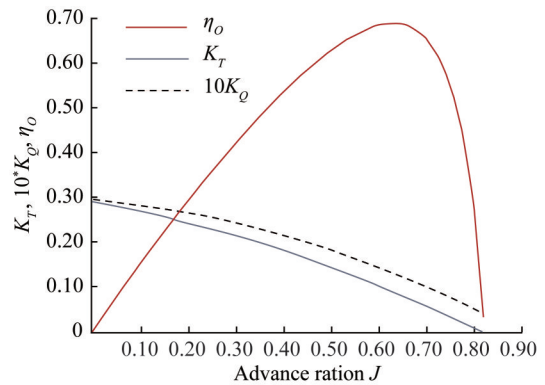


Figure 21 Propeller open-water characteristics

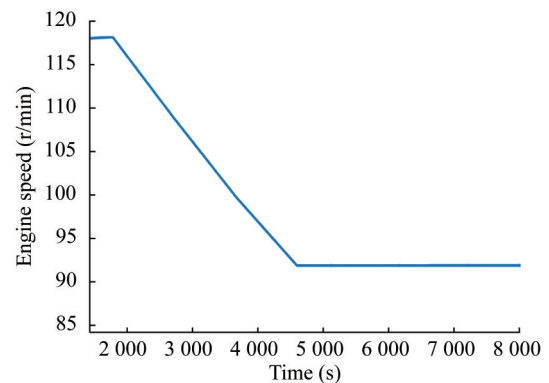


Figure 22 Engine speed as monitored onboard of the ship

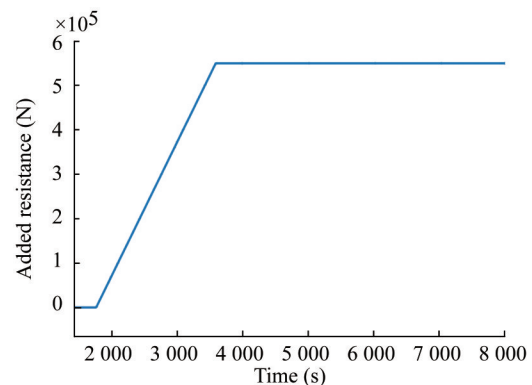


Figure 23 Added resistance in service condition estimated based on weather and ship condition

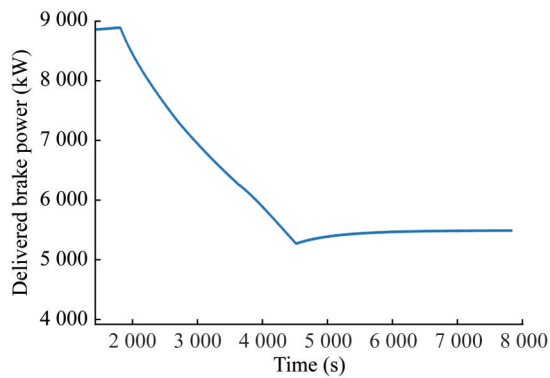


Figure 24 Simulation of the engine power output

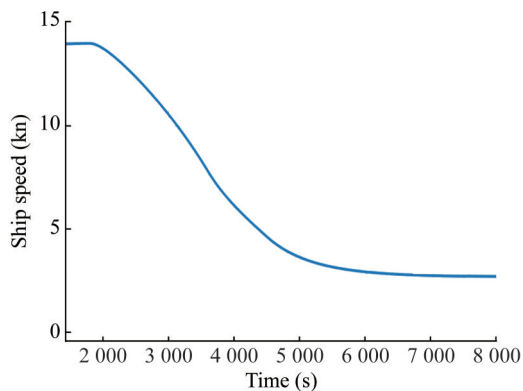


Figure 25 Simulation of the ship speed during this process

6 Conclusion

In this study, a dynamic model accounting for the interactions between the hull, propeller, and engine is set up and implemented in MATLAB Simulink to simulate a ship's fuel consumption during unsteady operation. In this model, the ship resistance and propeller characteristics are required as input. The diesel engine is modelled by a first-order transfer function with a delayed response and its performance is calibrated with the data from the manufacturer's catalogue. A governor is applied to maintain the pre-set engine's rotational speed and to control the engine fuel rate. In addition, a slope limiter is employed to approximate the actual engine operation during engine acceleration.

Using this model and the correlated software, the influence of using P or PI governor on fuel consumption is investigated. It is noted that using PI governor can achieve the commanded engine speed accurately, while the P governor fails to do so. When a slope limiter is implemented, a significant reduction in fuel consumption is observed, as compared with the case without such a limiter, owing to the lower acceleration of the engine speed which results in lower fuel input to the engine. Therefore, by limiting the acceleration of the engine, considerable savings on fuel consumption can be achieved, with a slight increase in travelling time. Additionally, the dynamic process of ship

acceleration, represented by the trace of engine operating point presented in the engine envelope, clearly demonstrated that the propeller curve will become heavier in this manoeuvre. The findings of this study are rather different from what earlier studies showed, despite that very similar model has been implemented to conduct the same case study.

After validation, the established model is applied to simulate the case of a real ship encounters harsh seaway condition. Simulation result show that the dynamic process of ship speed decreasing and the generated results are qualitatively in good agreement with monitored data. It should be noted that the current formulation is only a one degree of freedom (dof) model. We plan to extend it to multiple dof in the future and more validations and applications will be carried out.

Acknowledgement The first author would like to thank Professor Theotokatos of University of Strathclyde for his discussion and support of this study.

Competing interest The authors have no competing interests to declare that are relevant to the content of this article.

References

- Altosole M, Figari M (2011) Effective simple methods for numerical modelling of marine engines in ship propulsion control systems design. *Journal of Naval Architecture and Marine Engineering*, 8 (2): 129-147. <https://doi.org/10.3329/jname.v8i2.7366>
- Bendarenko O, Kashiwagi M (2010) Dynamic behaviour of ship propulsion plant in actual seas. *Marine Engineering*, 45, 1012-1016. <https://doi.org/10.5988/jime.45.1012>
- Ellis G (2012) Four types of controllers. In *Control System Design Guide*. 4th Ed, 97-119. <https://doi.org/10.1016/B978-0-12-385920-4.00006-0>
- Flagiello D, Esposito M, Di Natale F, Salo K (2021) A novel approach to reduce the environmental footprint of maritime shipping. *Journal of Marine Science and Application*, 20(2): 229-247. <https://doi.org/10.1007/s11804-021-00213-2>
- International Maritime Organization (2021) Guidelines for determining minimum propulsion power to maintain the manoeuvrability of ships in adverse conditions. London, International Maritime Organization. MEPC.1/Circ.850/Rev.3
- Karabulut UC, Özdemir YH, Barlas B (2020) Numerical study on the hydrodynamic performance of antifouling paints. *Journal of Marine Science and Application*, 19: 41-52. <https://doi.org/10.1007/s11804-020-00130-w>
- Kim S, Yun S, You Y (2021) Eco-friendly speed control algorithm development for autonomous vessel route planning. *Journal of Marine Science and Engineering*, 9(6): 583. <https://doi.org/10.3390/jmse9060583>
- Klein Woud H, Stapersma D (2002) Design of propulsion and electric power generation systems. IMarEST, Institute of Marine Engineering, Science and Technology, London
- Korotkin AI (2008) Added Masses of Ship Structures. e-ISBN 978-1-4020-9432-3, Springer Science + Business Media B.V. <https://doi.org/10.1007/978-1-4020-9432-3>
- Lanchukovsky VI (2009). Safe operation of marine power plants.

- Marine Engineering Practice Series. IMarEST, London.
- Liu S, Papanikolaou A (2012) On nonlinear simulation methods and tools for evaluating the performance of ships and offshore structures in waves. *Journal of Applied Mathematics*, 2012. <https://doi.org/10.1155/2012/563182>
- Liu S, Papanikolaou A (2020) Regression analysis of experimental data for added resistance in waves of arbitrary heading and development of a semi-empirical formula. *Ocean Engineering*, 206: 107357. <https://doi.org/10.1016/j.oceaneng.2020.107357>
- Liu S, Papanikolaou A, Shang BG (2022a) Critical review of the revised IMO-MEPC76 guidelines for assessing the minimum propulsion power of ships in view of the reduction of greenhouse gas emissions. *Ocean Engineering*. Vol. 249. 111011. <https://doi.org/10.1016/j.oceaneng.2022.111011>
- Liu S, Shang B, Chen H, Papanikolaou A (2022b) A fast and transparent method for setting powering margins in ship design. Proceedings of the ASME 2022 41st International Conference on Ocean, Offshore and Arctic Engineering, Hamburg, Germany. <https://doi.org/10.1115/OMAEE2022-78937>
- Liu S, Papanikolaou A (2023) Improving the empirical prediction of the added resistance in regular waves of ships with extreme main dimension ratios through dimensional analysis and parametric study. *Ocean Engineering*, 273: 113963. <https://doi.org/10.1016/j.oceaneng.2023.113963>
- MacPherson DM, Puleo VR, Packard MB (2007) Estimation of entrained water added mass properties for vibration analysis. SNAME New England Section
- MAN Diesel & Turbo (2012) Basic Principles of Ship Propulsion. Publication no.: 5510-0004-02ppr. Copenhagen, Denmark
- MAN Diesel & Turbo (2016) New Engine Control Technology for Improved Ship Acceleration. *Diesel Facts*. 2/2016
- Mizythras P, Boulougouris E, Theotokatos G (2018) Numerical study of propulsion system performance during ship acceleration. *Ocean Engineering*, 149: 383-396. <https://doi.org/10.1016/j.oceaneng.2017.12.010>
- Mocerino L, Guedes Soares C, Rizzuto E, Balsamo F, Quaranta F (2021) Validation of an emission model for a marine diesel engine with data from sea operations. *Journal of Marine Science and Application*, 20(3): 534-545. <https://doi.org/10.1007/s11804-021-00227-w>
- Molland A, Turnock S, Hudson D (2011) Ship resistance and propulsion: practical estimation of propulsive power. Cambridge: Cambridge University Press. <https://doi.org/10.1017/9781316494196>
- Nahim HM, Younes R, Nohra C (2015) Complete modeling for systems of a marine diesel engine. *Journal of Marine Science and Application*, 14, 93-104. <https://doi.org/10.1007/s11804-015-1285-y>
- Papatzanakis G, Papanikolaou A, Liu S (2012) Optimization of routing considering uncertainties. *Journal of Marine Science and Application*, 11(1): 10-17. <https://doi.org/10.1007/s11804-012-1100-y>
- Schulten PJM (2005) The Interaction between diesel engines, ship and propellers during manoeuvring. PhD dissertation. Delft University Press
- Sherbaz S, Duan W (2012) Operational options for green ships. *Journal of Marine Science and Application*, 11, 335-340. <https://doi.org/10.1007/s11804-012-1141-2>
- Taskar B, Yum KK, Steen S, Pedersen E (2016) The effect of waves on engine-propeller dynamics and propulsion performance of ships. *Ocean Engineering*, 122: 262-277. <https://doi.org/10.1016/j.oceaneng.2016.06.034>
- Tillig F, Ringsberg JW (2019) A 4 DOF simulation model developed for fuel consumption prediction of ships at sea. *Ships and Offshore Structures*, 14(sup1): 112-120. <https://doi.org/10.1080/17445302.2018.1559912>
- Vettor R, Soares CG (2016) Development of a ship weather routing system. *Ocean Eng*, 123: 1-14. <https://doi.org/10.1016/j.oceaneng.2016.06.035>
- Xing-Kaeding Y, Papanikolaou A (2021) Numerical and experimental study on the steady and unsteady forward speed motion of a catamaran. Proc. 31st Int. Ocean and Polar Engineering Conf. Rhodes, Greece
- Xiros N (2002) Robust control of diesel ship propulsion. Springer London
- Zeraatgar H, Ghaemi MH (2019) The analysis of overall ship fuel consumption in acceleration manoeuvre using hull-propeller-engine interaction principles and governor features. *Polish Maritime Research*, 26(1): 162-173. <https://doi.org/10.2478/pomr-2019-0018>